Proc. SPIE, Vol. 10228, Paper 102280E (2017)
DOI: 10.1117/12.2265671. SPIE Copyright
Author prepared version

Modeling of silicon in femtosecond laser-induced modification regimes: accounting for ambipolar diffusion

Thibault J.-Y. Derrien* and Nadezhda M. Bulgakova

HiLASE Centre, Institute of Physics AS CR, Za Radnicí 828/5, 25241 Dolní Břežany, Czech Republic

ABSTRACT

During the last decades, femtosecond laser irradiation of materials has led to the emergence of various applications based on functionalization of surfaces at the nano- and microscale. Via inducing a periodic modification on material surfaces (band gap modification, nanostructure formation, crystallization or amorphization), optical and mechanical properties can be tailored, thus turning femtosecond laser to a key technology for development of nanophotonics, bionanoengineering, and nanomechanics. Although modification of semiconductor surfaces with femtosecond laser pulses has been studied for more than two decades, the dynamics of coupling of intense laser light with excited matter remains incompletely understood. In particular, swift formation of a transient overdense electron-hole plasma dynamically modifies optical properties in the material surface layer and induces large gradients of hot charge carriers, resulting in ultrafast charge-transport phenomena. In this work, the dynamics of ultrafast laser excitation of a semiconductor material is studied theoretically on the example of silicon. A special attention is paid to the electron-hole pair dynamics, taking into account ambipolar diffusion effects. The results are compared with previously developed simulation models, and a discussion of the role of charge-carrier dynamics in localization of material modification is provided.

1. INTRODUCTION

Laser-induced modification of materials is one of the key technologies for the development of photonic applications. The modification phenomenon itself is extremely complicated and can proceed by different routes with different consequences through laser-induced melting[1] followed by amorphization and/or crystallization, nanostructure formation,[2] nanoparticle formation, ablation[3] and, as found recently, band-gap modification.[4]

Homogeneous, heterogeneous, and non-thermal melting. Starting from a certain laser pulse energy, a laser-irradiated material experiences melting of a superficial surface layer within the electron-phonon coupling time. For nanosecond laser irradiations, pump-probe experiments[1,5] demonstrate the formation of a melting front evolving from the surface towards the bulk of the material, so-called *heterogeneous melting*.[6] At ultrashort laser pulses, as the melting front velocity cannot be faster than the speed of sound in the irradiated material (close to 5,000 m/s in Si), overheating of the material can occur resulting in fluctuations of the local lattice temperature at the melting front.[7] Similarly to metals,[8] in silicon so-called *homogeneous melting* can develop via nucleation of homogeneously distributed melting centers, located below the surface of the irradiated material in the regime of critical kinetic limit of the melting front.[7] Hence, both surface and sub-surface melting phenomena can transiently happen upon laser irradiation, depending on the applied laser fluence and pulse duration.[9]

Ultrafast excitation of semiconductors at fluences above the damage threshold proceeds through a highly reflective, metal-like phase upon the development of a dense, overcritical electron-hole plasma.[10] If a significant percent (∼10-15%) of the valence electrons is excited to the conduction band, such strong electronic excitation is almost immediately followed by bond softening, leading to lattice destabilization and the appearance of non-thermal phase transitions (ultrafast or *non-thermal melting*) on a sub-ps time scale[11,12]

Subsurface overheating and volumetric ablation at nanosecond laser irradiation. For nanosecond irradiation regimes, the possibility of sub-surface (volumetric) nucleation of the vapor phase with consequences in explosive boiling (phase explosion) has been proven.[13–17] The mechanism is the following. Laser light is

*derrien@fzu.cz, phone +420-314007709; www.hilase.cz

Proc. SPIE, Vol. 10228, Paper 102280E (2017)
DOI: 10.1117/12.2265671. SPIE Copyright
Author prepared version

Refs	2-γ absorption σ_2 [m.W^{-1}]	Effective mass m^*[-]	e-ph coupling τ_c [fs]	Collision time ν^{-1} [fs]
Sabbah et al[48]	6.8×10^{-11}	$0.15 - 0.20$	260 ± 30	32 ± 5
Sokolowski et al*[10]	45×10^{-11}	0.18	-	1.1
Sjodin et al[21]	10×10^{-11}	-	240 ± 30	-
Bulgakova et al[36]	↑	0.18†	↑	1.27
Bristow et al[49]	1.86×10^{-11}	-	-	-
Reitze et al[50]	34.6×10^{-11}	0.18	-	
Choi et al[51]	2×10^{-11}	0.18	500	-
Fischetti et al[52]	-	-	-	~ 10 fs

Table 1: List of free parameters used in several modeling studies for the laser wavelength of $\lambda = 800$ nm. *Laser wavelength was $\lambda = 625$ nm in this study. †: In this study, electron-hole pair binding was also calculated explicitly via solving the Poisson equation.

absorbed by electrons whose thermalization with material lattice can be considered to occur instantaneously as compared with pulse duration. Although at certain conditions equilibrium between free electrons and lattice can be violated,[18] normal vaporization from the surface dominates at relatively low laser fluences.[13–15] With increasing laser fuence, vaporization of material from the surface cools down the surface while a subsurface layer may experience heating close to the thermodynamic critical temperature. As a consequence, swift homogeneous nucleation of the vapor phase and growing of the vapor bubbles result in the rupture of the superheated layer into a mixture of vapor and liquid droplets. However, the question on subsurface melting while the surface stays solid is still debated.[19,20]

Material modification with femtosecond lasers. In the regimes of femtosecond laser irradiation, the situation is different. As the electron-lattice thermalization time is considerably larger as compared to pulse duration (for silicon, it is of several picoseconds, depending on laser-excited plasma density),[21] electrons absorbing laser radiation are gaining high kinetic energies, while lattice stay cold during irradiation time.[10,22–28] As a whole, at ultrashort laser pulses, non-equilibrium electron dynamics dominate over thermal effects in band gap materials.[21,29–35] The resulting material modification and its localization strongly depend on the dynamics of excited electrons wherever it can be observed, at the surface or *below the surface level*.

At the spatial scale of the laser spot size (typically from several to dozens micrometers), the hydrodynamic approach is an efficient way to describe the carrier dynamics and to quantitatively analyze the available experimental measurements.[36–43] In particular, continuum modeling allows to study the excitation dynamics,[30,39,41,44–47] with interpreting numerically the pump-probe reflectivity measurements available in literature. However, the most of continuum models suffer from the necessity of using free parameters such as carrier collision frequency or the two-photon absorption rates. Such parameters are usually derived from experimental studies but they are varied in a rather wide range from one to another work (see Tab. 1). As often several adjusting parameters are introduced to a model while sensitivity of continuum simulations to them is very high, this limits predictability of material modification as function of the laser irradiation parameters.

To make an attempt of overcoming this difficulty, we have performed a study using a two-temperature model aimed at describing the dynamics of electron-hole pairs of femtosecond-laser irradiated silicon.[30,45,46] The description is mainly based on the well-established macroscopic formulation of *van Driel et al*,[53,54] where the ambipolar diffusion of electron-hole pairs is described using a reduced mobility coefficient. The model whose details are presented below allows to calculate the transient dynamics of the reflectivity as a function of time and laser parameters. A similar approach was recently used[47] for normally incident beams with sample reflectivity to be accounted only for the parameters on the surface of the excited material. In our case, a multilayer reflectivity model is applied[10,30,45,55,56] which integrates the modification of refractive index over the laser-excited layer of a material as a function of time. Monitoring of the balance of the laser energy distribution between the kinetic and potential energy channels is also performed in simulations.

Proc. SPIE, Vol. 10228, Paper 102280E (2017)
DOI: 10.1117/12.2265671. SPIE Copyright
Author prepared version

2. MODELING THE TRANSIENT EXCITATION OF SILICON

The model detailed in this part is based on the description of the carrier dynamics using the ambipolar diffusion formalism, where the quasi-neutrality of charge carriers is assumed. In the ambipolar diffusion approach, the densities of the conduction-band (CB) electrons N_e and electron-hole pairs N_{e-h} are taken equal:

$$N_e \equiv N_{e-h}.$$

It is also assumed that the temperatures of electrons and holes are also equal:

$$T_e \equiv T_{e-h}.$$

If to separately consider the electrons and holes (e.g., when electron photoemission and its consequences are of interest), the ambipolar diffusion should be explicitly described as the electrostatic interaction between the conduction electrons and the holes via solving the Poisson equation.[36,57,58] In the present work, a simpler formulation is used as developed by *van Driel*.[53] The energy transport due to gradients of carrier density and temperature is also added in the present simulations.

2.1 Calculations of the optical response

As the inhomogeneity of the electron density profile influences the sample reflectivity,[55] its value R is calculated using the multilayer reflectivity model

$$R = |r_{0,N}|^2 .$$

Here N is the number of considered layers, which are thin enough to assume that the carrier density is only slightly varying across the layer (the latter is typically equal to the numerical cell size). The reflectivity $r_{j,k}$ between layers j and k is calculated by the recurrent relation as

$$r_{j,k} = \frac{r_{j,j+1} + r_{j+1,k} e^{2i\phi_{j+1}}}{1 + r_{j,j+1} r_{j+1,k} e^{2i\phi_{j+1}}}.$$

The phase ϕ_{j+1} of the monochromatic light in a layer $j+1$ of thickness h_{j+1} is expressed as $\phi_{j+1} = \frac{2\pi h_{j+1}}{\lambda} \times \sqrt{\varepsilon_{j+1}}$. The coefficient $r_{j,j+1}$ is given by the angle- and polarization-dependent Fresnel coefficients.[59,60] For s polarization, one has

$$r^{(s)}_{j,j+1}(\theta) = \frac{\sqrt{\varepsilon_j}\cos\theta - \sqrt{\varepsilon_{j+1} - \varepsilon_j \sin^2\theta}}{\sqrt{\varepsilon_j}\cos\theta + \sqrt{\varepsilon_{j+1} - \varepsilon_j \sin^2\theta}}. \quad (1)$$

where ε_j and ε_{j+1} are the dielectric permittivities of the laser-excited Si in the layers j and $j+1$ respectively; θ is the angle of incidence of the laser wave on the sample surface. Note that this formulation is valid for relatively low values of incidence angles. For p polarization, it reads as

$$r^{(p)}_{j,j+1}(\theta) = \frac{\varepsilon_{j+1}\cos\theta - \sqrt{\varepsilon_j}\sqrt{\varepsilon_{j+1} - \varepsilon_j \sin^2\theta}}{\varepsilon_{j+1}\cos\theta + \sqrt{\varepsilon_j}\sqrt{\varepsilon_{j+1} - \varepsilon_j \sin^2\theta}}. \quad (2)$$

It is important to mention that convergence of the sample reflectivity can be obtained if using a regular fine mesh below the surface until a certain depth where the gradients of the excited matter parameters are becoming small. In deeper regions of the sample, an irregular grid may be used with a progression in size smaller than 1% for two neighboring cells.

The dynamic change of the refractive index is described by taking into account collective response of electrons as well as the transient response of the molten material via using the following formalism. The transient optical response of electrons is described via the Drude-like dielectric permittivity[10]

$$\varepsilon^*_{\mathrm{Si}}(N_{e-h}) = 1 + [\varepsilon_{\mathrm{Si}}(\omega, T_{\mathrm{Si}}) - 1]\frac{N_0 - N_{e-h}}{N_0} - \frac{\omega^2_{pe}(N_{e-h})}{\omega^2\left(1 + i\frac{\nu}{\omega}\right)},$$

Proc. SPIE, Vol. 10228, Paper 102280E (2017)
DOI: 10.1117/12.2265671. SPIE Copyright
Author prepared version

where $\omega_{pe} = \sqrt{\frac{N_{e-h}e^2}{m_e m^* \varepsilon_0}}$ is the plasma frequency, ν is the electron collision frequency chosen to be equal to a constant which can be adjusted to better fit experimental data,[36] N_0 is the density of valence electrons in the unexcited material state, and m^* is the effective mass of electrons in Si.[10,48] The free-carrier heating is also described by a Drude model.[10,36,61]

Both solid and liquid Si have a temperature-dependent dielectric permittivity $\varepsilon_{\mathrm{Si}}(\omega, T_{\mathrm{Si}})$. Thus, two models have been used jointly, based on the works of *Jellison et al.*[62,63]

2.2 Calculations of the electron-hole pair density N_{e-h}

The evolution of the density of the electron-hole (e-h) pairs with accounting for their transport is calculated via solving the continuity equation in the form

$$\frac{\partial N_{e-h}}{\partial t} + \boldsymbol{\nabla} \cdot \boldsymbol{J}_{e-h} = G_{e-h} + R_{e-h}. \tag{3}$$

The ambipolar diffusion current $\boldsymbol{J}_{e-h}$ can be described by assuming that the Fermi integrals are close[53] to 1

$$\boldsymbol{J}_{e-h} = -D_{e-h} \times \left[\boldsymbol{\nabla} N_{e-h} + \underbrace{\frac{N_{e-h}}{2T_{e-h}} \boldsymbol{\nabla} T_{e-h} + \frac{2N_{e-h}}{k_B T_{e-h}} \boldsymbol{\nabla} E_g}_{*} \right]. \tag{4}$$

In this and following equations, the curly brackets marked by asterisk $(*)$ indicate the terms which were neglected in our previous studies for simplicity reasons.[30,45,64] The ambipolar diffusion coefficient D_{e-h} is given by[54]

$$D_{e-h} = \frac{2k_B T_{e-h}}{e} \times \frac{\mu_e \times \mu_h}{\mu_e + \mu_h}. \tag{5}$$

As proposed by *van Driel*,[53] a harmonic average is taken for the free electron and hole conductivities to describe the electron-hole pairs diffusion coefficient D_{e-h}. Interestingly, the mobility can be strongly reduced during the femtosecond laser interaction.[65] As we also would like to match the mobility with experimental measurements, we keep the mobilities to be constant but ten times reduced as compared with the normal conditions: $\mu_e = 0.015$ $\mathrm{m}^2/(\mathrm{V{\cdot}s})$ for electrons and $\mu_h = 0.0045$ $\mathrm{m}^2/(\mathrm{V{\cdot}s})$ for holes.[36]

By combining Eqs. (3) and (4), we obtain

$$\frac{\partial N_{e-h}}{\partial t} + \boldsymbol{\nabla} \cdot \left(-D_{e-h} \times \left[\boldsymbol{\nabla} N_{e-h} + \underbrace{\frac{N_{e-h}}{2T_{e-h}} \boldsymbol{\nabla} T_{e-h} + \frac{2N_{e-h}}{k_B T_{e-h}} \boldsymbol{\nabla} E_g}_{*} \right] \right) = \tag{6}$$
$$= G_{e-h} + R_{e-h}.$$

More details can be found in the paper by Young et al.,[66] where, interestingly, it was shown that the independent-particle Boltzmann transport theory disregarding temperature gradients[67,68] overestimates the values of the ambipolar diffusion coefficient. Note that we also disregard the change of the band gap, keeping it constant in these simulations, while in future works its shrinking and collapse is planned to be accounted for describing non-thermal and thermal melting effects. In the present study, the band gap energy of silicon E_g is taken to be equal to that at 300 K, $E_g^0 = 1.12$ eV.

Proc. SPIE, Vol. 10228, Paper 102280E (2017)
DOI: 10.1117/12.2265671. SPIE Copyright
Author prepared version

2.3 Energy transport equation: taking into account the ambipolar diffusion

The transport of energy by e-h pairs can be calculated by solving the energy balance equation in the form[53,54]

$$C_{e-h}\frac{\partial T_{e-h}}{\partial t}+\underbrace{\boldsymbol{\nabla}\cdot\left[4k_BT_{e-h}\times\boldsymbol{J_{e-h}}\right]}_{*}=\boldsymbol{\nabla}\left[\kappa_{e-h}\boldsymbol{\nabla}T_{e-h}\right]+S_{e-h}. \tag{7}$$

where $C_{e-h}=\frac{3}{2}k_BN_{e-h}$ is the classical limit of the heat-capacity of electrons. The flux of the e-h pairs $\boldsymbol{J_{e-h}}$ is given by Eq. (4). The thermal conductivity reads as

$$\kappa_{e-h}=\frac{2k_B^2T_{e-h}N_{e-h}\left(\mu_e+\mu_h\right)}{e} \tag{8}$$

Note that, in this case, the electron mobility μ_e is not averaged as heat conductivity depends on the electron collision frequency and, hence, is not directly governed by the electron-hole interaction field. In other words, the thermal diffusivities of electrons and holes are additive.[53,54]

Finally, the energy transport equation (7) can be rewritten as

$$C_{e-h}\frac{\partial T_{e-h}}{\partial t}-\underbrace{\boldsymbol{\nabla}\cdot\left[4k_BT_{e-h}\times D_{e-h}\times\left[\boldsymbol{\nabla}N_{e-h}+\frac{N_{e-h}}{2T_{e-h}}\boldsymbol{\nabla}T_{e-h}+\frac{2N_{e-h}}{k_BT_{e-h}}\boldsymbol{\nabla}E_g\right]\right]}_{*}= \tag{9}$$

$$=\boldsymbol{\nabla}\left[\kappa_{e-h}\boldsymbol{\nabla}T_{e-h}\right]+S_{e-h}+C.$$

where $\boldsymbol{\nabla}E_g$ is the band gap energy gradient which, as mentioned above, is disregarded here.

2.4 Electron-lattice coupling and screening

The electron-hole coupling is given by the expression

$$C=-\gamma_{e-ph}(T_{e-h}-T_{\mathrm{Si}})$$

where $\gamma_{e-ph}=\frac{C_{e-h}}{\tau_{e-ph}}$. Screening of electron-phonon coupling at high free electron densities[21,69] was experimentally measured[70] and considered theoretically[30] with the maximum coupling time $\tau_{e-ph}^{\max}$ of 2 ps:

$$\tau_{e-ph}^{-1}=\left(\tau_{e-ph}^{\mathrm{screening}}\right)^{-1}+\left(\tau_{e-ph}^{\max}\right)^{-1} \tag{10}$$

The density-dependent electron-phonon coupling time is[21]

$$\tau_{e-ph}^{\mathrm{screening}}=\tau_0\left[1+\left(\frac{N_{e-h}}{N_{\mathrm{crit}}}\right)^2\right], \tag{11}$$

where the critical carrier density for screening $N_{\mathrm{crit}}=6.02\times10^{21}$ cm^{-3} and $\tau_0=240$ fs.

The lattice temperature is calculated by solving the heat-flow equation

$$C_{\mathrm{Si}}\frac{\partial T_{\mathrm{Si}}}{\partial t}=\boldsymbol{\nabla}\left(\kappa_{\mathrm{Si}}\boldsymbol{\nabla}T_{\mathrm{Si}}\right)+\gamma\left(T_e-T_{\mathrm{Si}}\right) \tag{12}$$

accounting for the transport of heat in the excited-solid and in the hot-liquid layer. Both the heat capacity C_{Si} and the thermal conductivity κ_{Si} of silicon both depend on the liquid density fraction η in the laser-excited volume and were calculated here as $C_{\mathrm{Si}}(T_{\mathrm{Si}})=(1-\eta)\,C_{\mathrm{Si}}^{(s)}(T_{\mathrm{Si}})+\eta C_{\mathrm{Si}}^{(l)}(T_{\mathrm{Si}})$ and $\kappa_{\mathrm{Si}}(T_{\mathrm{Si}})=(1-\eta)\,\kappa_{\mathrm{Si}}^{(s)}(T_{\mathrm{Si}})+\eta\kappa_{\mathrm{Si}}^{(l)}(T_{\mathrm{Si}})$. For non-molten (solid) silicon, the heat capacity $C_{\mathrm{Si}}^{(s)}$ and the thermal conductivity $\kappa_{\mathrm{Si}}^{(s)}$ are given by[71] $C_{\mathrm{Si}}^{(s)}$[J/(kg·K)]$=10^3\times(0.899e^{5.455\times10^{-5}\times T_{\mathrm{Si}}}-0.959e^{-0.004218\times T_{\mathrm{Si}}})$ and $\kappa_{\mathrm{Si}}^{(s)}$[W/(m·K)]$=1.585\times10^5T_{\mathrm{Si}}^{-1.23}$,[5,72] respectively. For the liquid state, the corresponding parameters are[73] $C_{\mathrm{Si}}^{(l)}(T_{\mathrm{Si}})$[J/(m$^3\cdot$K)] $=2.633\times10^6$ and[74] $\kappa_{\mathrm{Si}}^{(l)}(T_{\mathrm{Si}})$[W/(m·K)]$=50.2+29.3\times10^{-3}\,(T_{\mathrm{Si}}-T_m)$. The melting temperature T_m of silicon is 1687 K at normal pressure.[75] The melting process is considered here by keeping the local temperature constant at T_m until the internal energy increase reaches the melting enthalpy[26] $\Delta H_m=4.2\times10^9$ J/m^3.

Proc. SPIE, Vol. 10228, Paper 102280E (2017)
DOI: 10.1117/12.2265671. SPIE Copyright
Author prepared version

2.5 Excitation rates of electron-hole pairs

The description of free-carrier generation takes into account excitation of electrons from the valence band (VB) to the conduction band (CB) via one- and two-photon absorption and collisional (impact) ionization with probabilities σ_1, σ_2, and δ_{II} respectively:[53]

$$G_{e-h} = \left(\frac{\sigma_1 I}{\hbar\omega} + \frac{\sigma_2 I^2}{2\hbar\omega} + \delta_{\text{II}} N_{e-h} \right) \frac{N_0^\dagger - N_{e-h}}{N_0^\dagger}.$$

Here $N_0^\dagger$ is the atomic density of unexcited material. Recombination of the e-h pairs is considered as the Auger process which is calculated as

$$R_{e-h} = N_{e-h} / \left[\tau_{\text{AR}} + \left(C_{\text{AR}} N_{e-h}^2 \right)^{-1} \right]$$

with $C_{\text{AR}} = 3.8 \times 10^{-43}$ m^6/s.[76,77] At high free electron densities $\sim 10^{21}$ cm^{-3}, the characteristic recombination time τ_{AR} saturates at the level of 6 ps.[78]

Laser light attenuation upon beam propagation toward the sample depth is described by the Beer-Lambert law with accounting for the energy losses in the photo-ionization events and inverse bremsstrahlung absorption:

$$\frac{\mathrm{d}I}{\mathrm{d}z} = -(\sigma_1 I + \sigma_2 I^2 + \alpha_{\text{B}} I).$$

The intensity at the surface is determined via transiently changing reflectivity:

$$I(t, x, z = 0) = [1 - R(t)]\, I_0(x, t).$$

The bremsstrahlung absorption coefficient is calculated as $\alpha_{\text{B}} = \frac{4\pi}{\lambda} \text{Im} \sqrt{\varepsilon_{fcr}}$ wherein $\varepsilon_{fcr} = 1 - \frac{\omega_{pe}^2}{\omega^2 \left(1 + i \frac{\nu}{\omega}\right)}$.

The energy source is written as in the work by *Bulgakova et al.*[36] In the general case, it should account for the temporal change of the band gap E_g:

$$\begin{aligned} S_{e-h} = \Bigg[& (\hbar\omega - E_g) \frac{\sigma_1 I}{\hbar\omega} + (2\hbar\omega - E_g) \frac{\sigma_2 I^2}{2\hbar\omega} \\ & - \delta_{\text{II}} E_g N_{e-h} \Big] \times \frac{N_0^\dagger - N_{e-h}}{N_0^\dagger} + \underbrace{\alpha_{\text{B}} I}_{*} + E_g R_{e-h} - \frac{3}{2} k_B T_{e-h} \frac{\partial N_{e-h}}{\partial t} \\ & \underbrace{- N_{e-h} \frac{\partial E_g}{\partial t} - \left(E_g - E_g^0 \right) \times \frac{\partial N_{e-h}}{\partial t}}_{*} \end{aligned}$$

which, however, is not considered here. Note that in works[30,64] the inverse bremsstrahlung absorption was disregarded.

2.6 Boundary conditions

The electron photoemission from the sample surface is not taken into account and the computational domain in the sample is sufficiently large to secure that the charge-carrier flux is equal to zero at the remote boundary. Hence, the condition $\boldsymbol{J}_{e-h} = -D_{e-h} \boldsymbol{\nabla} N_{e-h} = 0$ is applied for both the surface and the remote boundary of the sample. The similar boundary conditions are imposed on the heat transfer by electron-hole pairs and silicon lattice: $\boldsymbol{Q}_i = -\kappa_i \boldsymbol{\nabla} T_i = 0$.

2.7 Selection of the free parameters

The optical mass m^* is related to the electron temperature. The values close to $m^* = 0.18$ describe accurately several sets of experimental data.[10,21,48] Hence we choose this value for our study. It is known that the mobilities of charge carriers in highly-excited semiconductors decrease as compared to unexcited state.[65,66,79,80] As was mentioned above, the mobilities μ_e and μ_h were set constant but reduced.[36]

Proc. SPIE, Vol. 10228, Paper 102280E (2017)
DOI: 10.1117/12.2265671. SPIE Copyright
Author prepared version

Parameter	Symbol	Value	Unit	References
Laser wavelength	λ	800	nm	
Pulse duration	τ	100	fs	
Angle of incidence	θ	0°	-	
Polarization	-	linear	-	
Collision frequency	ν^{-1}	~ 1.25	fs	[36]
Electron effective mass	m^*	0.18	-	[10,21,48]
Electron mobility	μ_e	0.015	m/(V·s)	[36]
Hole mobility	μ_h	0.0045	m/(V·s)	[36]

Table 2: Laser irradiation parameters and the properties of the excited electrons and holes used in the present simulations.

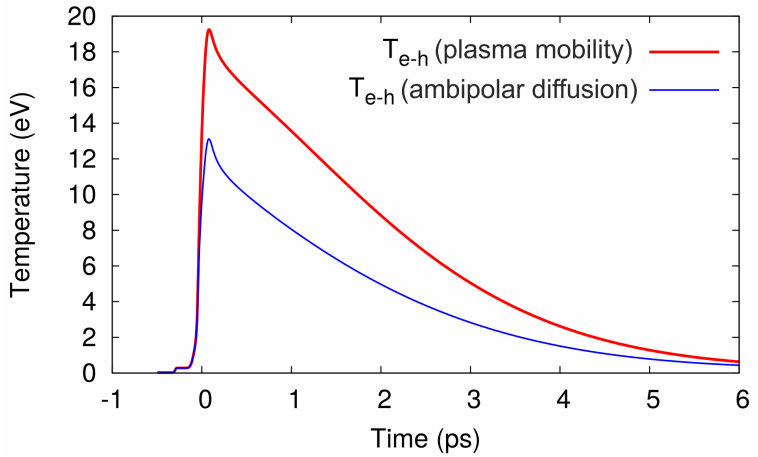

Figure 1: Evolution of the electron temperature with time during and after the laser pulse (laser fluence $F_0 = 0.8$ J/cm^2). Two models of mobility/diffusion are compared. In a "plasma mobility" model, ambipolar diffusion is disregarded and the electron mobility is used instead in the form $\mu_e = \frac{q}{m\nu}$ (see[30,45,64]). The data marked "ambipolar diffusion" are obtained with the improved model described in Section 2.

3. RESULTS OF NUMERICAL SIMULATIONS

The model equations were calculated using finite-difference implicit numerical scheme. For the aim of comparing the improved model, described in Section 2, with other models, this section considers parameters that were treated historically in a previous series of papers.[30,36,45] In particular, the maximum free electron temperature of the order of 6-7 eV was reported for the peak fluence of 0.8 J/cm^2 and 100 fs pulse duration.[36]

3.1 Transient maximum of carrier kinetic energy

In a number of previous studies,[30,39,41,51,64,81] laser-induced excitation of e-h pairs in silicon was considered with accounting for exchange of energy with lattice. However, the energy transported due to diffusion of e-h pairs was underestimated. A more accurate description of the ambipolar diffusion was given in sophisticated studies involving charge separation and solving the Poisson equation, that is laborious and computer-resources consuming.[36,57,58] In this section, we compare the two approaches and, in addition, take into account the transport of carriers induced by the gradients of the electron temperature.[53,54] Laser and charge-carrier parameters used in simulations are summarized in Table 2.

Figure 1 presents the evolution of the conduction electron temperature as a function of time at the laser fluence of 0.8 J/cm^2. When disabling any electronic transport (not shown here), T_{e-h} reaches the level of 30 eV (~348,000 K). In the "plasma mobility" model, the charge carrier diffusion due to only the e-h density gradient was taken into account (Eq. (6)), the electron mobility was used for calculating the diffusion term, and the heat

Proc. SPIE, Vol. 10228, Paper 102280E (2017)
DOI: 10.1117/12.2265671. SPIE Copyright
Author prepared version

transport (Eq. (9)) was governed only by the electron heat conductivity.[30,45] This model yields the maximum electron temperature ∼19 eV which then decreases due to mainly the electron heat conduction (Fig. 1, red line).

When using the ambipolar diffusion model detailed in Section 2 with, however, disregarded the band-gap shrinking, the maximum electron temperature drops to ∼13 eV for $F_0 = 0.8$ J/cm^2 (Fig. 1, blue line). Such considerable drop originates from the more accurate description which accounts self-consistently for the diffusive transport of the carrier mass and energy in the model (indicated by brackets with asterisks in the equations of Section 2). Such electron temperature is still approximately two times higher in comparison with 6-7 eV reported by *Bulgakova et al.*[36] for the same irradiation regime. Note that, in the latter cited work, a depletion of a surface layer from electrons due to electron photoemission was taken into account. As the result, the local charge-carrier energy at the surface can occur smaller than in the present study due to less efficient absorption in the surface layer depleted from electrons. However, this does not mean that the overall energy balance is considerably different. According to simulations,[36] depletion of electrons takes place from a surface layer of only few nanometers thick while, in the rest part of the sample, the carrier dynamics can be similar to that observed in the present study. Nevertheless, it should be pointed that the drift-diffusion transport of charge carriers and associated energy transport can also be affected by the transient photoemission-induced electric field, the effect which calls for further studies.

3.2 Monitoring the energy balance

Figure 2(a)-(b) presents the energy balance evolution as a function of time. The energy balance was monitored by two ways. Using the dynamic reflectivity, the absorbed laser fluence was integrated over time. At the same time, the fractions of the absorbed laser fluence (potential energy of electrons, or $N_e(t) \times E_g$; kinetic energy of electrons; energy transferred from the electrons to the lattice) and their redistribution in time and depth were calculated during simulations.

For relatively low laser peak fluences [Fig. 2(a), $F_0 = 0.12$ J/cm^2, near the melting threshold], the potential energy of the excited electrons is ∼ 27.5% of the absorbed laser energy while ∼ 55% of it is consumed by free electrons in the form of their kinetic energy increase. The Auger recombination process, which is very slow in this regime (see Section 2.5), gradually transfers the potential energy back to the kinetic energy (almost unseen at the timescale of 3 ps) which then is transferred to the lattice. At high fluences [Fig. 2(b), $F_0 = 0.8$ J/cm^2, well above the ablation threshold], 35% of the laser energy are back-reflected while the rest energy is distributed as follows. Only 5% of the incident energy are spent for the excitation of electrons from VB to CB and the rest 60% are consumed for the thermal heating of the electrons, in their turn transferring the energy to the lattice with time. This figure demonstrates a very good conservation of the total laser energy in the used numerical scheme. It shows that, the fraction of the absorbed laser energy, which is spent for the electron heating, considerably increases with laser fluence that, according to the simulations, results in the efficient electron-lattice energy exchange already at subpicosecond tome scale. At high laser fluences it can plausibly lead to *thermal melting shortly after the laser pulse*, already at femtosecond time scale. However, a deeper insight is required for taking into account such phenomena as, on one hand, superheating of solid material at ultrafast energy coupling[8] and, on the other hand, non-thermal melting.[12]

3.3 A possibility of sub-surface melting?

In the simulations, due to strong gradients of the electron-hole density N_{e-h} and temperature T_{e-h} in the laser-excited silicon layer, the electron-phonon coupling becomes most efficient at certain depth beneath the sample surface where $N_{e-h} \leq N_{\text{crit}}$, see Eq. (11). Accounting for electron lattice thermalization according to Eq. (11) leads most probably to overestimating the electron-phonon coupling time when the carrier density N_{e-h} considerably exceeds the critical carrier density for screening N_{crit}.[21,30,70] As liquid silicon has metal-like optical properties ($\Re e\,(\varepsilon_{l\text{-Si}}) \sim -13$ for 800 nm wavelength), the temporal dynamics of the sample reflectivity can be affected during the melting process by appearance a metal-like liquid silicon layer. According to preliminary simulations, such sub-surface melting generates oscillations in the temporal reflectivity profile due to interfering of probe pulse with its parts reflected from moving melting interfaces.[3,59] To provide a more physically grounded model of material melting, the N_{e-h}-dependent electron-phonon coupling time was limited to the experimentally proven maximum value of 2 ps[30,70] (see Eq. (10)). Note that the refractive index of Si is also dependent on the

Proc. SPIE, Vol. 10228, Paper 102280E (2017)
DOI: 10.1117/12.2265671. SPIE Copyright
Author prepared version

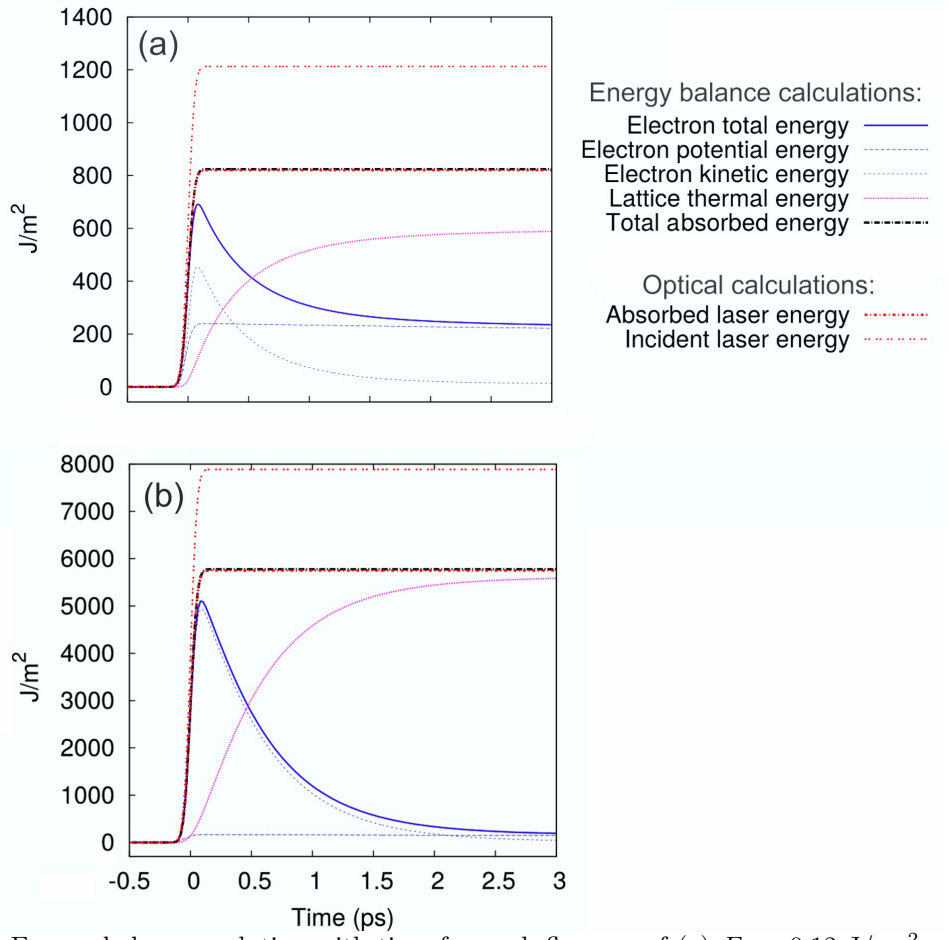

Figure 2: (a-b) Energy balance evolution with time for peak fluences of (a) $F_0 = 0.12$ J/cm^2 and (b)$F_0 = 0.8$ J/cm^2. The laser pulse maximum is at $t = 0$.

lattice temperature that was taken into account in the simulations, using adjusting functions to the available experimental data.[62,63] The simulations for direct comparison with pump-probe experiments on dynamic silicon reflectivity are under progress and will be published elsewhere.

4. CONCLUSION

The continuum modeling approach for the description of the ultrashort-laser excitation dynamics of semiconductors has been improved with accounting for the ambipolar diffusion of free carriers. Its application for silicon has been developed and tested. Comparisons with previously obtained simulation results demonstrate a high importance of the ambipolar diffusion terms in the model, both in the equation for the free-carrier generation and transport and in the energy balance equation, which are widely neglected for simplicity. The numerical implementation of the presented model has proven accurate energy conservation at relatively low and high laser fluences. To account for the contribution of free-carrier density gradients inside the sample to the transient sample reflectivity, a multilayer model of reflectivity is used, opening the way for the direct comparison of modeling results with temporal evolution of material reflectivity under real experimental conditions. Contributions of screening of the electron-phonon coupling as well as of homogeneous, heterogeneous, and non-thermal melting to transient reflectivity dynamics of silicon is under study.

Proc. SPIE, Vol. 10228, Paper 102280E (2017)
DOI: 10.1117/12.2265671. SPIE Copyright
Author prepared version

Acknowledgments

TJYD was supported by the Marie Sklodowska-Curie Action (MSCA) Individual fellowship (QuantumLaP project No. 657424) of Horizon 2020. This work was also supported by the European Regional Development Fund and the state budget of the Czech Republic (project BIATRI: CZ.02.1.01/0.0/0.0/15_003/0000445) and by the Ministry of Education, Youth and Sports (Programs NPU I - project no. LO1602, and Large Infrastructures for Research, Experimental Development and Innovations - projects no. LM2015086 and "IT4Innovations National Supercomputing Center – LM2015070", computational project Quantum-1st-LaP.).

REFERENCES

[1] Wood, R. F. and Gilles, G. E., "Macroscopic theory of pulsed-laser annealing. i. thermal transport and melting," *Phys. Rev. B* **23**, 6 (1981).

[2] Birnbaum, M., "Semiconductor surface damage produced by ruby lasers," *J. Appl. Phys.* **36**, 3688 (1965).

[3] Bäuerle, D., [*Laser Processing and Chemistry*], Springer-Verlag, 4th edition ed. (2011).

[4] Healy, N., Mailis, S., Bulgakova, N. M., Sazio, P. J. A., Day, T. D., Sparks, J. R., Cheng, H. Y., Badding, J. V., and Peacock, A. C., "Extreme electronic band-gap modification in laser crystallized silicon optical fibres," *Nat. Mater.* **13**, 1122 (2014).

[5] Wood, R. and Geist, G., "Modeling of nonequilibrium melting and solidification in laser-irradiated materials," *Phys. Rev. B* **34**, 4 (1986).

[6] Vechten, J. V., Tsu, R., Saris, F., and Hoonhout, D., "Reasons to believe pulsed laser annealing of si does not involve simple thermal melting," *Phys. Lett. A* **74**, 6 (1979).

[7] Ivanov, D. and Zhigilei, L., "Kinetic limit of heterogeneous melting in metals," *Phys. Rev. Lett.* **98**, 195701 (2007).

[8] Lin, Z., Leveugle, E., Bringa, E. M., and Zhigilei, L. V., "Molecular Dynamics Simulation of Laser Melting of Nanocrystalline Au," *The Journal of Physical Chemistry C* **114**, 5686 (2010).

[9] Kumada, T., Akagi, H., Itakura, R., Otobe, T., and Yokoyama, A., "Femtosecond laser ablation dynamics of fused silica extracted from oscillation of time-resolved reflectivity," *J. Appl. Phys.* **115**, 103504 (2014).

[10] Sokolowski-Tinten, K. and von der Linde, D., "Generation of dense electron-hole plasmas in silicon," *Phys. Rev. B* **61**, 2643 (2000).

[11] Shank, C. V., Yen, R., and Hirlimann, C., "Femtosecond-time-resolved surface structural dynamics of optically excited silicon," *Physical Review Letters* **51**(10), 900 (1983).

[12] Rousse, A., Rischel, C., Fournaux, S., Uschmann, I., Sebban, S., Grillon, G., Balcou, P., Forster, E., Geindre, J., Audebert, P., Gauthier, J., and Hulin, D., "Non-thermal melting in semiconductors measured at femtosecond resolution," *Nature* **410**, 65–68 (2001).

[13] Kelly, R. and Miotello, A., "Comments on explosive mechanisms of laser sputtering," *Appl. Surf. Sci.* **96-98**, 205 (1995).

[14] Kelly, R. and Miotello, A., "Does normal boiling exist due to laser-pulse or ion bombardment?," *J. Appl. Phys.* **87**, 3177 (2000).

[15] Bulgakova, N. M.; Bulgakov, A. V., "Pulsed laser ablation of solids: transition from normal vaporization to phase explosion:," *Appl. Phys. A* **73**, 199 (2001).

[16] Yoo, J. H., Jeong, S. H., Mao, X. L., Greif, R., and Russo, R. E., "Evidence for phase-explosion and generation of large particles during high power nanosecond laser ablation of silicon," *Appl. Phys. Lett.* **76**, 783 (2000).

[17] Craciun, V., Bassim, N., Singh, R. K., Craciun, D., Hermann, J., and Boulmer-Leborgne, C., "Laser-induced explosive boiling during nanosecond laser ablation of silicon," *Appl. Surf. Sci.* **186**, 288 (2002).

[18] Marine, W., Bulgakova, N. M., Patrone, L., and Ozerov, I., "Insight into electronic mechanisms of nanosecond-laser ablation of silicon," *J. Appl. Phys.* **103**, 094902 (2008).

[19] Zhvavyi, S. and Zykov, G., "Simulation of composition modification in ZnSe by nanosecond radiation of excimer laser," *Appl. Surf. Sci.* **254**(20), 6504–6508 (2008).

[20] Bulgakova, O. A., Bulgakova, N. M., and Zhukov, V. P., "A model of nanosecond laser ablation of compound semiconductors accounting for non-congruent vaporization," *Appl. Phys. A* **101**, 53 (2010).

Proc. SPIE, Vol. 10228, Paper 102280E (2017)
DOI: 10.1117/12.2265671. SPIE Copyright
Author prepared version

[21] Sjodin, T., Petek, H., and Dai, H.-L., "Ultrafast carrier dynamics in silicon: A two-color transient reflection grating study on a (111) surface.," *Phys. Rev. Lett.* **81**, 5664 (1998).

[22] Sokolowski-Tinten, K., Blome, C., Dietrich, C., Tarasevitch, A., von Hoegen, M. H., von der Linde, D., Caravelli, A., Squier, J., and Kammler, M., "Femtosecond x-ray measurement of ultrafast melting and large acoustic transients," *Phys. Rev. Lett.* **87**, 22 (2001).

[23] Kudryashov, S. I. and Emelyanov, V. I., "Band gap collapse and ultrafast cold melting of silicon during femtosecond laser pulse," *Journal of Experimental and Theoretical Physics Letters* **73**, 228 (2001).

[24] Sokolowski-Tinten, K., Blome, C., Blums, J., Cavalleri, A., Dietrich, C., Tarasevitch, A., Uschmann, I., Forster, E., Kammler, M., von Hoegen, M. H., and von der Linde, D., "Femtosecond X-ray measurement of coherent lattice vibrations near the Lindemann stability limit," *Nature* **422**, 287–289 (2003).

[25] Temnov, V. V., Sokolowski-Tinten, K., Zhou, P., and von der Linde, D., "Ultrafast imaging interferometry at femtosecond-laser-excited surfaces," *J. Opt. Soc. Am. B* **23**, 1954 (2006).

[26] Korfiatis, D., Thoma, K., and Vardaxoglou, J., "Conditions for femtosecond laser melting of silicon," *J. Phys. D- Appl. Phys.* **40**, 6803 (2007).

[27] Zijlstra, E., Kalitsov, A., Zier, T., and Garcia, M., "Squeezed thermal phonons precurse nonthermal melting of silicon as a function of fluence," *Physical Review X* **3**, 011005 (2013).

[28] Zijlstra, E. S., Kalitsov, A., Zier, T., and Garcia, M. E., "Fractional diffusion in silicon," *Advanced Materials* **25**, 5605 (2013).

[29] Hnatovsky, C., Shvedov, V., Krolikowski, W., and Rode, A., "Revealing local field structure of focused ultrashort pulses," *Phys. Rev. Lett.* **106**, 123901 (2011).

[30] Derrien, T. J.-Y., Krüger, J., Itina, T. E., Höhm, S., Rosenfeld, A., and Bonse, J., "Rippled area formed by surface plasmon polaritons upon femtosecond laser double-pulse irradiation of silicon," *Opt. Express* **24**, 29643 (2013).

[31] Ruggenthaler, M., Flick, J., Pellegrini, C., Appel, H., Tokatly, I. V., and Rubio, A., "Quantum-electrodynamical density-functional theory: Bridging quantum optics and electronic-structure theory," *Physical Review A* **90**, 012508 (2014).

[32] Zhang, P., Feist, J., Rubio, A., Garcia-Gonzalez, P., and Garcia-Vidal, F. J., "Ab initio nanoplasmonics: The impact of atomic structure," *Physical Review B* **90**, 161407 (2014).

[33] Apostolova, T., Huang, D. H., Alsing, P. M., McIver, J., and Cardimona, D. A., "Effect of laser-induced antidiffusion on excited conduction electron dynamics in bulk semiconductors," *Phys. Rev. B* **66**, 075208 (2002).

[34] Apostolova, T., Perlado, J., and Rivera, A., "Femtosecond laser irradiation induced-high electronic excitation in band gap materials: A quantum-kinetic model based on Boltzmann equation," *Nuclear Instruments and Methods in Physics Research Section B: Beam Interactions with Materials and Atoms* **352**, 167 (2015).

[35] Huang, D., Alsing, P. M., Apostolova, T., and Cardimona, D. A., "Coupled energy-drift and force-balance equations for high-field hot-carrier transport," *Phys. Rev. B* **71**, 195205 (2005).

[36] Bulgakova, N. M., Stoian, R., Rosenfeld, A., Hertel, I. V., Marine, W., and Campbell, E. E. B., "A general continuum approach to describe fast electronic transport in pulsed laser irradiated materials: The problem of Coulomb explosion," *Appl. Phys. A* **81**, 345 (2005).

[37] Chimier, B., Tikhonchuk, V., and Hallo, L., "Heating model for metals irradiated by a subpicosecond laser pulse," *Phys. Rev. B* **75**, 195124 (2007).

[38] Chimier, B., Utéza, O., Sanner, N., Sentis, M., Itina, T., Lassonde, P., Légaré, F., Vidal, F., and Kieffer, J. C., "Damage and ablation thresholds of fused-silica in femtosecond regime," *Phys. Rev. B* **84**, 094104 (2011).

[39] Tsibidis, G., Barberoglou, M., Loukakos, P., Stratakis, E., and Fotakis, C., "Dynamics of ripple formation on silicon surfaces by ultrashort laser pulses in subablation conditions," *Phys. Rev. B* **86**, 115316 (2012).

[40] Bulgakova, N. M., Zhukov, V. P., and Meshcheryakov, Y. P., "Theoretical treatments of ultrashort pulse laser processing of transparent materials: toward understanding the volume nanograting formation and "quill" writing effect," *Applied Physics B* **113**, 437 (2013).

[41] Tsibidis, G. D., Fotakis, C., and Stratakis, E., "From ripples to spikes: A hydrodynamical mechanism to interpret femtosecond laser-induced self-assembled structures," *Physical Review B* **92**, 041405 (2015).

Proc. SPIE, Vol. 10228, Paper 102280E (2017)
DOI: 10.1117/12.2265671. SPIE Copyright
Author prepared version

[42] Bulgakova, N. M., Zhukov, V., Meshcheryakov, Y. P., Gemini, L., Brajer, J., Rostohar, D., and Mocek, T., "Pulsed laser modification of transparent dielectrics: what can be foreseen and predicted in numerical experiments ?," *Journal of the Optical Society of America B* **11**, C8 (2014).

[43] Bulgakova, N. M. and Zhukov, V. P., [*Continuum Models of Ultrashort Laser-Matter Interaction in Application to Wide-Bandgap Dielectrics*], ch. Lasers in Materials Science, 101, Springer International Publishing (2014).

[44] Medvedev, N. and Rethfeld, B., "A comprehensive model for the ultrashort visible light irradiation of semiconductors," *J. Appl. Phys.* **108**, 103112 (2010).

[45] Derrien, T. J.-Y., Itina, T. E., Torres, R., Sarnet, T., and Sentis, M., "Possible surface plasmon polariton excitation under femtosecond laser irradiation of silicon," *J. Appl. Phys.* **114**, 083104 (2013).

[46] Levy, Y., Derrien, T. J.-Y., Bulgakova, N. M., Gurevich, E. L., and Mocek, T., "Relaxation dynamics of femtosecond-laser-induced temperature modulation on the surfaces of metals and semiconductors," *Appl. Surf. Sci.* **374**, 157 (2016).

[47] Rämer, A., Osmani, O., and Rethfeld, B., "Laser damage in silicon: energy absorption, relaxation and transport," *J. Appl. Phys.* **116**, 053508 (2014).

[48] Sabbah, A. and Riffe, D., "Femtosecond pump-probe reflectivity study of silicon carrier dynamics," *Phys. Rev. B* **66**, 165217 (2002).

[49] Bristow, A. D., Rotenberg, N., and van Driel, H. M., "Two-photon absorption and kerr coefficients of silicon for 850 - 2200 nm," *Appl. Phys. Lett.* **90**, 191104 (2007).

[50] Reitze, D., Zhang, T., Wood, W. M., and Downer, M. C., "Two-photon spectroscopy of silicon using femtosecond pulses at above-gap frequencies," *J. Opt. Soc. Am. B* **7**, 84 (1990).

[51] Choi, T. Y. and Grigoropoulos, C. P., "Plasma and ablation dynamics in ultrafast laser processing of crystalline silicon," *J. Appl. Phys.* **92**, 9 (2002).

[52] Fischetti, M. and Laux, S., "Monte carlo analysis of electron transport in small semiconductor devices including band-structure and space-charge effects," *Phys. Rev. B* **38**, 14 (1988).

[53] van Driel, H. M., "Kinetics of high-density plasmas generated in Si by 1.06- and 0.53-μm picosecond laser pulses," *Phys. Rev. B* **35**, 8166 (1987).

[54] Chen, J., Tzou, D., and Beraun, J., "Numerical investigation of ultrashort laser damage in semiconductors," *International Journal of Heat and Mass Transfer* **48**, 501 (2005).

[55] Vinet, J. Y., Combescot, M., and Tanguy, C., "Influence of the electron-hole density profile on the reflectivity of laser irradiated silicon," *Solid State Commun.* **51**, 171 (1984).

[56] Bulgakova, N. M., Stoian, R., and Rosenfeld, A., "Laser-induced modification of transparent crystals and glasses," *Quantum Electron.* **40**, 966 (2010).

[57] Bulgakova, N. M., Stoian, R., Rosenfeld, A., Hertel, I., and Campbell, E., "Electronic transport and consequences for material removal in ultrafast pulsed laser ablation of materials," *Phys. Rev. B* **69**, 054102 (2004).

[58] Silaeva, E. P., Vella, A., Sevelin-Radiguet, N., Martel, G., Deconihout, B., and Itina, T. E., "Ultrafast laser-triggered field ion emission from semiconductor tips," *New Journal of Physics* **15**, 089401 (2013).

[59] Born, M. and Wolf, E., [*Principles of Optics. Electromagnetic theory of propagation, interference and diffraction of light.*], Cambridge University Press, 7th edition ed. (1980).

[60] Jackson, J. D., [*Classical Electrodynamics*], Wiley, 3rd edition ed. (1999).

[61] Van Exter, M. and Grischkowsky, D., "Carrier dynamics of electrons and holes in moderately doped silicon," *Phys. Rev. B* **41**, 12140 (1990).

[62] Jellison, G. and Modine, F., "Optical absorption of silicon between 1.6 and 4.7 ev at elevated temperatures," *Appl. Phys. Lett.* **41**, 2 (1982).

[63] Jellison, G. E., "Optical constants for silicon at 300 and 10 K determined from 1.64 to 4.73 eV by ellipsometry," *J. Appl. Phys.* **53**, 3745 (1982).

[64] Derrien, T. J.-Y., Krüger, J., Itina, T. E., Höhm, S., Rosenfeld, A., and Bonse, J., "Rippled area formed by surface plasmon polaritons upon femtosecond laser double-pulse irradiation of silicon: the role of carrier generation and relaxation processes," *Applied Physics A* **117**, 77 (2014).

[65] Sjodin, T., Li, C.-M., Petek, H., and Dai, H.-L., "Ultrafast transient grating scattering studies of carrier dynamics at a silicon surface," *Chem. Phys.* **251**, 205 (2000).

[66] Young, J. F. and van Driel, H. M., "Ambipolar diffusion of high-density electrons and holes in Ge, Si, and GaAs: Many-body effects," *Phys. Rev. B* **26**, 2147 (1982).

[67] Kreuzer, H. J., [*Nonequilibrium thermodynamics and its statistical foundations*], vol. 1 (1981).

[68] van Driel, H. M., Leung, T. L. F., and Young, J. F., "Thermodiffusion of high-density electron-hole plasmas in semiconductors," *Phys. Rev. Lett.* **49**, 698 (1982).

[69] Yoffa, E. J., "Screening of hot-carrier relaxation in highly photoexcited semiconductors," *Phys. Rev. B* **23**, 1909 (1981).

[70] Harb, M., Ernstorfer, R., Dartigalongue, T., Hebeisen, C. T., Jordan, R. E., and Miller, R. J. D., "Carrier relaxation and lattice heating dynamics in silicon revealed by femtosecond electron diffraction," *J. Phys. Chem. B* **110**, 25308 (2006).

[71] Okhotin, A. S., Pushkarskii, A. S., and Gorbachev, V. V., [*Thermophysical properties of semiconductors*], Atom Publication House (1972).

[72] Glassbrenner, C. J. and Slack, G. A., "Thermal conductivity of silicon and germanium from 3k to the melting point," *Phys. Rev.* **134**, A1058 (1964).

[73] Desai, P., "Thermodynamic properties of iron and silicon," *J. Phys. Chem. Ref. Data* **15**, 967 (1986).

[74] Magna, A. L., Alippi, P., Privitera, V., Fortunato, G., Camalleri, M., and Svensson, B., "A phase-field approach to the simulation of the excimer laser annealing process in Si," *J. Appl. Phys.* **95**, 4806 (2004).

[75] Rhim, W.-K. and Ohsaka, K., "Thermophysical properties measurement of molten silicon by high-temperature electrostatic levitator: density, volume expansion, specific heat capacity, emissivity, surface tension and viscosity," *J. Cryst. Growth* **208**, 313 (2000).

[76] Huldt, L., Nilsson, N., and Svantesson, K., "The temperature dependence of band-to-band auger recombination in silicon," *Appl. Phys. Lett.* **35**, 10 (1979).

[77] Svantesson, K. and Nilsson, N., "The temperature dependence of the auger recombination coefficient of undoped silicon," *Journal of Physics C: Solid State Physics* **12**, 5111 (1979).

[78] Combescot, M. and Bok, J., "Comment on "time-resolved reflectivity measurements in silicon"," *Phys. Rev. Lett.* **51**, 519 (1983).

[79] Gabriel, M. M., Kirschbrown, J. R., Christesen, J. D., Pinion, C. W., Zigler, D. F., Grumstrup, E. M., Mehl, B. P., Cating, E. E., Cahoon, J. F., and Papanikolas, J. M., "Direct imaging of free carrier and trap carrier motion in silicon nanowires by spatially-separated femtosecond pump–probe microscopy," *Nano Lett.* **13**, 1336 (2013).

[80] Mouskeftaras, A., Chanal, M., Chambonneau, M., Clady, R., Utéza, O., and Grojo, D., "Direct measurement of ambipolar diffusion in bulk silicon by ultrafast infrared imaging of laser-induced microplasmas," *Appl. Phys. Lett.* **108**, 041107 (2016).

[81] He, S., Nivas, J. J., Anoop, K., Vecchione, A., Hu, M., Bruzzese, R., and Amoruso, S., "Surface structures induced by ultrashort laser pulses: Formation mechanisms of ripples and grooves," *Appl. Surf. Sci.* **353**, 1214 (2015).